Parametric Analysis of Battery-Electric Rotorcraft Configurations to Fly on Mars

Vishal Youhanna*†, Leonard Felicetti* and Dmitry Ignatyev*
*School of Aerospace, Transport, and Manufacturing,
Cranfield University,
College Rd, Cranfield, Wharley End,
Bedford MK43 0AL, UK.
vishal.youhanna@cranfield.ac.uk – leonard.felicetti@cranfield.ac.uk – d.ignatyev@cranfield.ac.uk
† Corresponding Author

Abstract

The success of NASA's Ingenuity Helicopter promises that the future exploration of Mars will include aerobots in line with rovers and landers. However, Ingenuity lacks long-range endurance and scientific payload capacity because of its small and elementary design. In the series of optimised Martian drone concepts development, we introduced in this paper - an initial sizing of rotary eVTOL design configurations based on the performed parametric analysis for hover and vertical climb using simplified rotorcraft momentum theory, for a set of more challenging requirements for a Martian aerobot mission and sized to fit into the maximum spacecraft aeroshell limit. A tandem rotor configuration was found to be the most efficient configuration, whereas a conventional single main rotor configuration with small diameters manifested the poorest performance.

1. Introduction

There is a growing interest in the exploration of Mars. To make future exploration missions sustainable, designing, developing, testing, and manufacturing an aerobot adapted for the low-pressure atmosphere of Mars is an extremely important problem. Mars was only closely explored via unmanned orbiters, landers, and rovers, until 2021. The idea of using unmanned aerial vehicles has been around for quite a time as it has offered numerous advantages such as increased speed, range, avoidance of obstacles, and field of view over a traditional surface rover [1]. In the past, planetary exploration research interest majorly has been limited to light-than-air airships or fixed wings planes, due to the higher technical complexity of the rotating wing aerobots. However, in recent years more interest has emerged in this subject due to the technological advances made in the development of a variety of terrestrial drones for commercial use. Based on this advancement in drone technologies, the first and only aerobot has been constructed, launched, and landed on Mars in the year 2021, which is currently in an operational state.

One possible solution is to use low Reynolds number specialized airfoils to design and study an eVTOL fixed-winged Mars drone. Winged aircraft have better endurance due to increased lift per power unit, which in return prolongs the range of the mission. This would increase the size of the aerobot, which could benefit in terms of carrying larger science payloads and in providing increased surface area for solar panels. But contrarily, wings also add complexity (if requiring a folding mechanism) and extra weight during VTOL. Therefore, a generic parametric study is deemed necessary to answer the question of whether the addition of wings to the Martian rotorcraft is beneficial overall, and if so, then in what configurations. In Martian environment settings, a relationship between rotor disk area and power required for hover and vertical climb of rotorcraft is theoretically analysed using simplified momentum theory. Hence, the initial sizing of a combination of fixed wing and rotorcraft will be considered next for forward flight to analyse the pros and cons of such a hybrid design for a whole flight regime.

2. Background

The features that make Mars different from Earth, also present a unique set of design challenges for a rotorcraft, majorly because of its atmospheric conditions. Even though Martian gravity is only about 38% of Earth's gravity, the Martian average atmospheric density is about 100 times lower than Earth's atmospheric density [2]. Therefore, the rotors would be operating at extremely low Reynolds numbers, even lower than 5000 for a small-scale helicopter. However, the Mach number will be significantly higher (M>0.4) because of the higher tip speed required (due to lower density) and the speed of sound on Mars is only about 72% of the speed of sound on Earth. This low-Reynolds-number, high-Mach-number flow condition on the blade imposes severe constraints on the rotor design. One of the most critical abilities needed to sustain the flight of a Martian drone is to minimise/reject the heat generated by the propulsion system while generating the required lifting thrust, which is extremely difficult, considering the low Reynolds numbers involved [3]. Added to the above constraints is the size limitation of aeroshell (4.5m diameter max) that would transport the aerobot to Mars [4]. All these challenges for flying a rotating wing aerobot on Mars have been a major question mark for the feasibility of the project in the past, until April 2021.

The feasibility of flying an unmanned rotorcraft on Mars is hundred percent because as of today we have evidentiary data from NASA's Ingenuity Mars Helicopter that landed on Mars in February 2021, and as of April 2023, it has completed its short autonomous pre-commanded 51st flight. In total it has flown for 91.4 minutes, covering 11.7 km, reaching altitudes as high as 18 m, and flying with a ground speed of as fast as 6.5 m/s. During these test flights, Ingenuity has transitioned from the Technology Demonstration phase to the Operations Demonstration phase, to showcase how future rovers and aerial surveyors can work together [5]. Now based on the Mars Helicopter design, a more sophisticated aerobot for flying on Mars can be produced.

3. Research Gap and Mission Statement

In-situ exploration of Mars is dominated by landers & rovers, which have limitations. An Aerobot can overcome such limitations, but it experiences design challenges. Ingenuity Helicopter has showcased the flight ability of an unmanned aerial vehicle on Mars, but the design of the helicopter has limitations such that it lacks the endurance, range, and science payload capacity due to its small size and basic design. These limitations reduce its ability to perform scientific exploration missions that would require long-distance flights, higher scientific payload, a sophisticated communication system, or a powerful propulsion system for high-altitude flights.

For this reason, we aim to enhance the design of such kinds of aerobots by proposing and setting a new set of more challenging requirements for a Martian aerobot mission and consequently propose a new design for the rotorcraft. We also consider that the aerobot shall be realistically sized to fit into the maximum aeroshell limit of 4.5 m diameter, assuming that the launch and re-entry technology will not drastically change in the next few decades.

For this mission location, SW (South West) Melas Basin of Melas Chasma, located at 9.81° south latitude and 76.47° west longitude, part of the Valles Marineris canyon system on Mars is assumed. Valles Marineris has been marked a location of interest by scientists for quite a while, including the Curiosity rover and the Mars 2020 mission landing site, because of the geological and life science Mars exploration goals, but has been avoided due to its rocky and rugged landscape. However, the implication of improved navigational planetary landing technology, and aerobots' capability of obstacle avoidance by flying over them, makes the in-situ exploration of this site promising in the near future [3]. An aerobot can help to generate a high-resolution aerial mapping of the area and can mark potential experimental/sample collection points for future rover missions. The mission primarily aims to obtain high-quality images of the areas scouted and effectively communicate them to a rover (eventually belonging to the same mission) or ground control station (Earth).

One possible solution to enhance the capability of Ingenuity Helicopter is to add fixed wings to the design. In the past, several fixed-wing aircrafts with VTOL capability have been proposed for Mars Exploration, which had either rigid [6]-[11] or foldable [12][16] body configurations, and recently one VTOL Inflatable winged configuration has been researched on as well [14]. Winged aircraft have better endurance due to increased lift per power unit, which in return prolongs the range of the mission. Using the same rotor blades of Ingenuity or the optimized airfoil of the advanced Mars Science Helicopter [15], a VTOL Foldable Fixed Winged Mars drone can be designed and studied. This would increase the size of the aerobot, which could benefit in terms of carrying bulkier science payloads and in providing increased surface area for solar panels. However, the downside of a larger aerobot is that it would need to be either transported as a standalone payload in the spaceship to Mars or be packaged with a smaller rover/lander, due to the limitation of the current aeroshell size. It might require a folding mechanism to be fitted into the aeroshell. Therefore, a generic parametric study of rotorcraft

configurations is deemed necessary to answer the question of whether the addition of wings to the Martian rotorcraft is beneficial overall, and if so, then in what configurations.

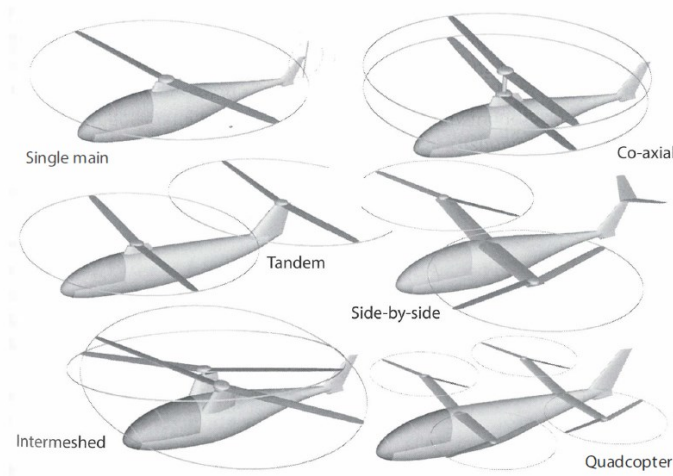## 4. Methodology for Power Requirement Analysis of Rotorcrafts

Fig. 1 Existing rotorcraft configurations (Image from [16]). Single main rotor is a conventional setting with one large rotor and a tail rotor. Coaxial rotors are two equal sized rotors rotating opposite to each other on the same axis. Similarly, tandem rotors and side-by-side rotors use two contrarotating rotors positioned in the longitudinal and horizontal axes, respectively. Intermeshing design has two contrarotating rotors that use a single gearbox and avoid collision. Quadcopter and other multicopter design use multiple pairs of smaller contrarotating rotors.

4.1 Conventional Rotorcraft VTOL (single main on Fig. 1)

The most important aspect of a reusable Martian aerobot flight on Mars is VTOL due to the unavailability of runways, and that is solely dependent on the rotary propulsion system of the rotorcraft. The momentum theory provides an estimate of the power consumption of the rotor for hover, vertical climb, and forward flight. Momentum theory assumes that the rotor blades when spinning act as an actuator disk of negligible thickness with a disk area S. There are a few other assumptions such as uniform airflow throughout the rotor disc and an instantaneous imparting of energy to the airflow, along with ignoring of airfoil profile drag losses, tip losses, and residual rotational velocities. To address these losses, a measure (or figure) of merit, M, is introduced into the calculation which is a ratio of ideal power to actual power ($M=P_{ideal}/P_{actual}$) and acts as a rotor efficiency parameter. Equation (1) calculates power for the vertical climb (V_{climb}) or hover (when the velocity of the climb is zero), for a conventional helicopter. This equation is taken from the book of Raymer D. [16], who based on terrestrial empirical data has included additional fudge factors to make the analysis reasonably practical. The total power is inclusive of the power required to drive the tail rotor. The ratio of power required by the tail rotor to the power required by the main rotor ($P_{tail\ rotor}/P_{main\ rotor}$) is between 0.14 to 0.22, as tail rotors are typically about 15-20% of the main rotor's diameter.

$$P_{(V_{climb}\ or\ hover)} = \left[\left(\frac{fW}{M}\sqrt{\frac{fW/S}{2\rho}}\right) + \frac{WV_{Climb}}{2}\right]\left[\frac{(1 + P_{tail\ rotor}/P_{main\ rotor})}{\eta_{mechanical}}\right] \qquad (1)$$

Where:

P = Power required; W = helicopter weight; S = rotor disk area; M = measure of merit; Vclimb = climb speed (= 0 for hover);   f = adjustment for downwash on the fuselage (typically f = 1 .03); ρ = Martian Air Density; $\eta_{mechanical}$ = mechanical losses adjustment due to driving of tail rotor (typically $\eta_{mechanical}$ = 0.97)

4.2 Coaxial Rotorcraft VTOL (Fig. 1)

The purpose of the tail rotor in a conventional helicopter setting is to provide a torque balance, by generating equal but confronting thrust force to the strong torque force produced as a byproduct of the spinning of the main rotor. However, if in place of a tail rotor, another equal-sized but contrarotating rotor is installed in the lift-producing direction, the problem of torque gets resolved with the added benefit of extra lift produced by this second rotor. One of the configurations of a twin rotors setting is a coaxial rotorcraft, where two rotors are installed to the same shaft in mechanically a more complicated hub setting. At first guess, it would be presumed that the lift force is doubled but because of the closeness of the two rotors, a part of the lift is lost due to airflow wake interference. Theoretically, a 100 percent overlapping case is of a coaxial rotor system with a zero vertical gap, where the overlapping interference factor (K_{ov}) increases the power consumption by a factor of $\sqrt{2}$ ($\sim$ 41% increase) when compared to two isolated (independent of the effect of the upper rotor wake) rotors [17]. The no vertical spacing coaxial setting is termed as an equivalent single rotor when it is equated to a system of smaller twin rotors with the same total thrust and total projected area (i.e., disk loading) because these share the same rotor solidity [18]. Rotor solidity, σ, is the ratio of the total area of the rotor blades to the total disk area. In the real world, the coaxial rotor hub system has a mechanical separation between the two rotors, and as this vertical separation increases the wake of the top rotor contracts and affects less area of the lower rotor, thus reducing the overlapping interference factor. For a large separation (LS), typically around 10% of the rotor diameter, the K_{ov} becomes 1.281 when uniform disk loading is assumed [17][18]. Therefore, Eq. (1) is adjusted for a coaxial rotor system of two equal-sized rotors such that the total rotorcraft weight (thrust) is shared equally, and the total power is multiplied by the overlapping interference factor (K_{ov}) to form Eq. (2). As there is no tail rotor but a second rotor, thus the ratio of power required by two equal-sized rotors ($P_{second\ rotor}/P_{main\ rotor}$) becomes 1.

$$P_{(V_{climb}\ or\ hover)} = \left[\left(\frac{fW}{(2\sqrt{2})M}\sqrt{\frac{fW/S}{2\rho}}\right) + \frac{WV_{Climb}}{2}\right]\left[\frac{2}{\eta_{mechanical}}\right][K_{ov}] \tag{2}$$

4.3 Tandem Rotorcraft and Side-by-side Rotorcraft VTOL (Fig. 1)

Another configuration of a twin rotors system is a tandem rotorcraft, where two equal-sized rotors are assembled longitudinally, one in front of the other on the fuselage. Theoretically, in this setting there can be up to 50% overlapping area, depending on the positional gap between the rotors; thus, the initial power analysis follows the same coaxial rotors power formula as stated in Eq. (2). However, the K_{ov} in a tandem setting is a function of the ratio (d/D), i.e., horizontal distance d between the two rotor axes to the rotor diameter D. For a case of rotors in the same plane (i.e., assumed no vertical gap between rotors), K_{ov} can be approximated using Eq. (3). In other cases, where the rotors are in separate planes and the portion of the lower rotor is working under the contracting wake of the upper rotor, the overlapping area must be determined first by numerical integration to find a solution to K_{ov}. Similarly, there are side-by-side configurations with overlapping rotors that could use this approach to estimate the total power required. One such configuration is of intermeshing rotors, known as synchropter, which has two counter-rotating rotors set at outward-tilting angles about fuselage width apart, driven by a single gearbox that ensures collision avoidance of the rotor blades with each other. Another subtype is transverse rotorcraft, such as tiltrotors and tiltwings, which contrary to tandem rotors are mounted horizontally on the tips of side wings or extended support frame of the fuselage, and have smaller rotors that do not overlap and act more like isolated rotors: essentially because these convert into forward propeller setting for the cruise flight [17][18].

$$K_{ov} = \left[\sqrt{2} - \frac{\sqrt{2}}{2}\left(\frac{d}{D}\right) + \left(1 - \frac{\sqrt{2}}{2}\right)\left(\frac{d}{D}\right)^2\right] \tag{3}$$

4.4 Isolated Rotors VTOL (e.g., Quadcopter in Fig. 1)

The value of overlapping interference factor K_{ov} changes from $\sqrt{2}$ to 1 when the same plane overlapping area between two equal-sized rotors transitions from full to zero: thus, acting as isolated rotors in the latter case. Although there can still be

a negligible amount of favorable or unfavorable interference despite no overlap of the rotors when there is a vertical separation, however, this can be ignored for the preliminary study cases [17][18]. For side-by-side configurations of multiple rotors with no overlap, Eq. (1) can be adjusted for a multirotor system of N number of equal-sized rotors such that the total rotorcraft weight (thrust) is equally shared by all, to form Eq. (4). As there is no tail rotor, thus the ratio of power required by the tail rotor to the power required by the main rotor ($P_{\text{tail rotor}}/P_{\text{main rotor}}$) simply is replaced by (N – 1) number of rotors.

$$P_{(V_{\text{climb or hover}})} = \left[\left(\frac{fW}{(N\sqrt{N})M}\sqrt{\frac{fW/S}{2\rho}}\right) + \frac{WV_{\text{Climb}}}{2}\right]\left[\frac{N}{\eta_{\text{mechanical}}}\right] \tag{4}$$

5. Methodology for the Initial Sizing of Battery-Electric Aircraft

The total maximum take-off aircraft weight (W_0) is comprised of empty weight (W_e), payload, and fuel. The weight of the fuel-burning aircraft decreases due to the burning of the fuel as it progresses through each segment of the flight, such as moving on the runway, taking off, ascending, cruising, and descending. The aircraft becomes lighter, and the drag varies accordingly, thus the initial sizing estimates include the integration of the calculation of each segment. Unlike fuel-burning aircraft, the battery mass of an electric aircraft does not change and therefore the integration of the various flight segments is not required. The fuel component of the total aircraft weight is replaced by the battery weight (W_b), and the required battery mass for each mission segment is developed using Eq. (5), expressed as the ratio battery mass to total aircraft mass (m_b/m), called Battery Mass Fraction (BMF). Eq. (5) includes the terms 'known run-time endurance (E)' and power used for flight segments such as V_{climb}, hover and forward flight of a rotorcraft. The total required aircraft BMF is then found as the sum of the different mission segment Battery Mass Fractions [16].

$$BMF = \frac{m_b}{m} = \frac{W_b}{W_0} = \frac{EP_{\text{used}}}{E_{sb}\eta_{b2s}m} \tag{5}$$

Where:
m_b = battery mass; m = aircraft total mass; W_b = battery weight; W_0 = aircraft total take-off weight; P_{used} = power required (Watt = W); E = known run time (hour = h); E_{s2b} = battery specific energy {W.h/kg}; η_{b2s} = total system efficiency from the battery to the motor output shaft (typically $\eta_{b2s} \sim 0.9$)

The total aircraft weight W_0 can be determined from Eq. (6), which is further modified to form the electric aircraft sizing Eq. (7) by including the total Battery Mass Fraction and empty weight W_e ratio [16]. The payload can be an instrument or a delivery object for an unmanned aircraft. Whereas, W_e includes everything other than payload or functional batteries such as propulsion system, aircraft structure, avionics, navigation and other essential equipment.

$$W_0 = W_e + W_b + W_{\text{payload}} \tag{6}$$

$$W_0 = \frac{W_{\text{payload}}}{1 + BMF_{\text{total}} + \frac{W_e}{W_0}} \tag{7}$$

The initial sizing equation can be used to start with rough first estimates of empty weight ratio from and payload weight statistical data, the calculated required BMF, to solve for the total weight, or by using known factors to find the unknown factor such as estimating the total weight and empty weight and calculated required BMF to solve for aircraft's payload capacity. This can be an iterative process until the calculation reaches a reasonable value to match the desired estimate to conduct preliminary design study.

6. Results and Analysis

6.1 Definition of parameters for analysis

The most important parameter for the initial power sizing analysis of rotorcraft is the air density at which it will generally fly the most. Mars' mean surface air density is 0.02 kg/m³ [19] which is quite an optimistic value, as it depends on the location, and altitude from the datum (sea level) and varies across seasons and time of the day. For the primary mission at SW Melas Chasma, which is about ~ 2 km below the datum, using The Mars Climate Database (Version 5.3) [20] the values of the regional air density at a flight time of 11th-hour local solar time [3] are estimated for the surface and the altitude of up to 1 km, spread across the one Martian year. The analysis produced a mean air density of 0.016 kg/m³.

Table 1   Parameters used in the V_{climb} and hover power analysis of different configurations of rotorcrafts

Parameter	Values			Unit
Mean Air Density	0.016			kg/m3
Speed of Sound	240.00			m/s
Limit of Max Rotor Blade Tip Speed	0.75			Mach
Mars Speed at Max Rotor Tip Speed	180.00			m/s
Max Forward Flight Speed	60.00			m/s
Average Vertical Climb V_{climb} Velocity	16.00			m/s
Aircraft MTOG Mass	20			kg
Aircraft MTOG Weight, W	74.42			N
Rotor Blade Diameter, Blade D	0.23	to	4.50	m
Rotor Disk Area, S	0.04	to	14.35	m2
Battery Specific Energy, E_{s2b}	230.00			W.h/kg
Measure (or figure) of Merit, M	0.7			
Mechanical efficiency factor, $\eta_{mechanical}$	0.97			
Fuselage downwash adjustement, f	1.03			
Helicopter P ratio ($P_{tail\ rotor}/P_{rotor}$)	0.18			
Coaxial P ratio ($P_{second\ rotor}/P_{main\ rotor}$)	1			
System efficiency from battery to motor (η_{b2s})	0.9			

The second defined parameter is the constraint set around the maximum size of the aerobot. For this mission, the protective heat shield that encapsulates spacecraft to transport the aerobot to Mars, called aeroshell, is the limiting factor. The maximum existing aeroshell size of diameter 4.5 m and height of ~ 2.2 m has been defined to design and analyse the possible Martian aerobot configurations. For preliminary design, the maximum rotor size would include a clearance from the internal wall of the aeroshell, however, a range of 0.23 m to 4.5 m of rotor diameter sizes is used in this parametric analysis.

The max forward velocity is set as 60 m/s, which is 1/4 of the average speed of sound (240 m/s) on Mars [3] and 1/3 of the max rotor tip speed permitted. For a rotorcraft to generate any lift on the retreating blade, the advancing blade must go possibly three times the helicopter's airspeed, but to avoid building up of transonic compression waves, the max tip speed of a rotor is limited to ~ 0.75 Mach [16]. The rotorcraft would aim to go up to 1 km in 1 minute, therefore the average vertical climb (V_{climb}) velocity is set at ~16 m/s. The total mass of the aerobot has been chosen to be 20 kg for the mission. The measure of merit, M, is typically from 0.6 to 0.8 [16], therefore a mean value of 0.7 is used. The battery specific energy

E_{s2b} used for V_{climb} BMF is 230 Wh/kg, based on a JPL technology forecast [4]. Table 1 provides the summary of the above-mentioned parameters used in the V_{climb} and hover power analysis of different configurations of rotorcrafts.

6.2 Conventional Helicopter Analysis

In Fig. 2 power required for the conventional helicopter is plotted against the increasing rotor disk diameter. The rotor disk area increases with the increase of rotor diameter, and in contrast, the disk loading (total weight divided by disk area, W/S) decreases. The lower the disk loading, the lesser the battery power required to hover or climb (i.e., the larger the power loading, W/P, permitted). However, a lower disk loading indicates a bigger rotor blade that adds to the weight, drag in forward flight, and tendency to encounter shocks on the advancing blade [16]. It can be noticed in the graph plot that smaller-sized rotors consume multiple times higher power than bigger rotors, and there is a dramatic decrease in power as the rotor disk diameter is increased. We have investigated and observed that this exponential decrement moves to the right while it slowly becomes stable when the total aerobot mass is increased. The helicopter required vertical climb power is slightly higher than the hover power, as expected due to the energy needed to generate vertical forward propulsion, but it can be noticed that as the rotor disk size increases the difference between the two power requirements amplifies gradually.
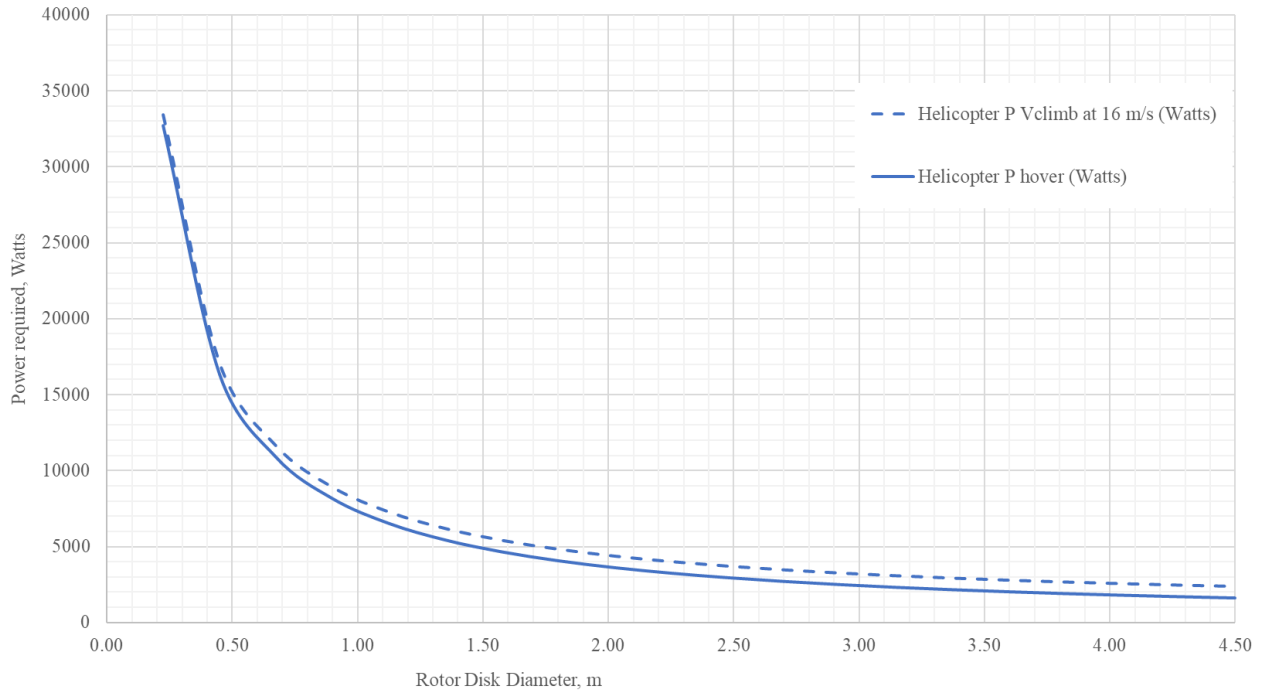

Fig. 2 20 kg Martian Conventional Helicopter - Power Required Vs Rotor Disk Diameter (Area)

6.3 Coaxial Rotorcraft Analysis

In Fig. 3 power required for the coaxial rotorcraft with large separation (LS) is plotted against the increasing rotor disk diameter. The power consumption of two equal-sized coaxial rotors is lower for smaller-sized rotors when compared to the conventional helicopter in Fig. 2. There is a difference of ~10k Watts for the required hover power between the conventional helicopter and coaxial rotorcraft at a rotor size of 0.23 m diameter. Similar to the helicopter power requirement trend, the LS coaxial vertical climb power is higher than the hover power, and with the increase of rotor disk diameter, the difference slowly increases; however, it can be noticed that this gap between the Vclimb power and hover power is greater than the gap observed in conventional helicopter power requirements. This implies that for vertical climb the coaxial rotorcraft will consume higher power when compared to the conventional setting.
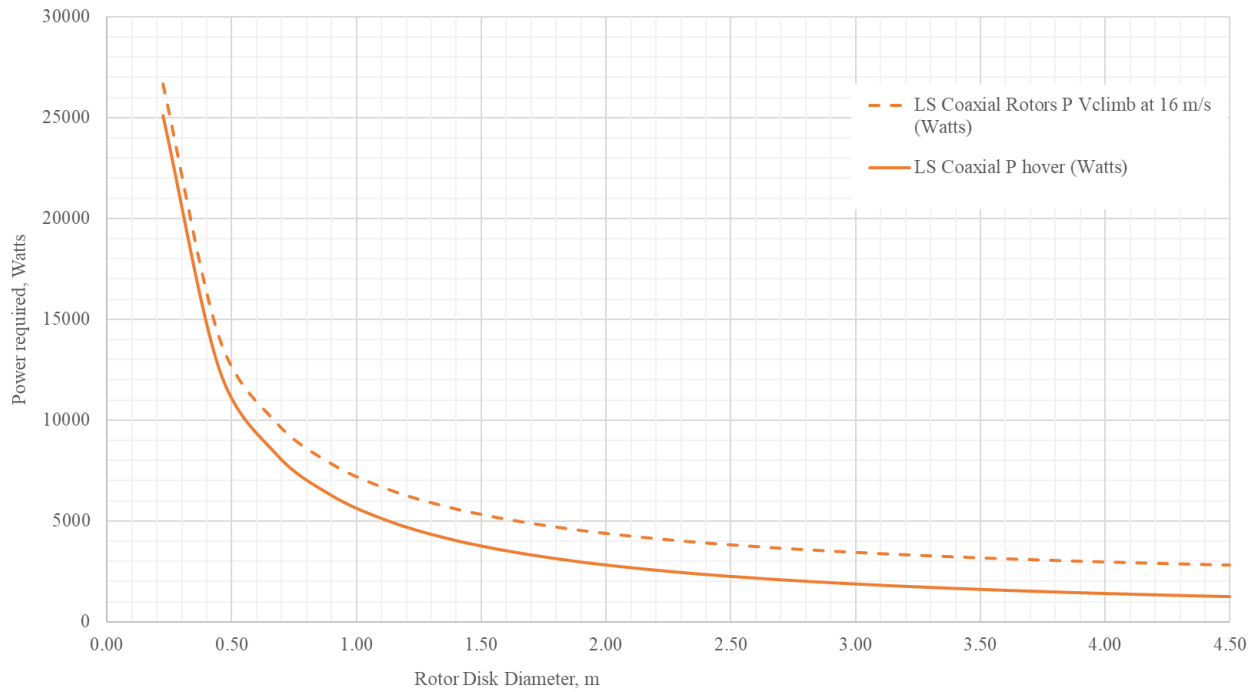
Fig. 3 20 kg Martian Coaxial Rotorcraft with Large Separation (LS) between rotors - Power Required Vs Rotor Disk Diameter (Area)

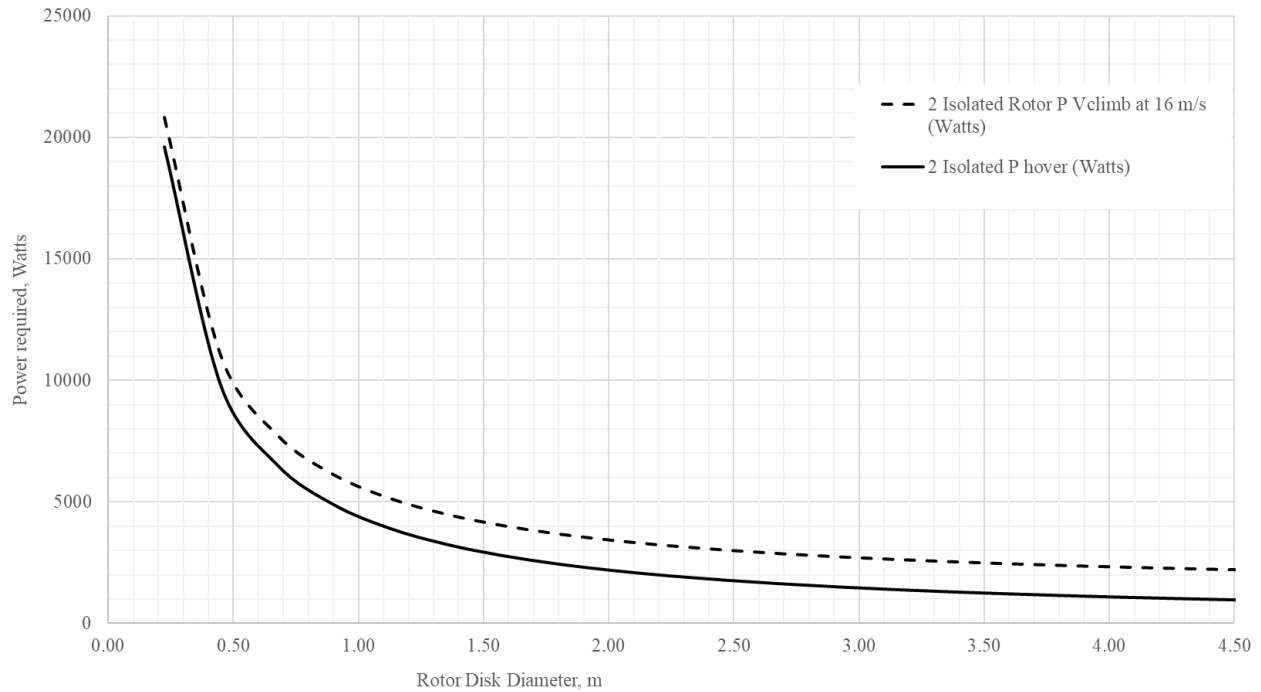## 6.4 Two Isolated Rotors Analysis

Fig. 4 20 kg 2 Isolated Rotors Rotorcraft - Power Required Vs Rotor Disk Diameter (Area)

In Fig. 4 power required for rotorcraft with 2 isolated rotors is plotted against the increasing rotor disk diameter. The power consumption of two equal-sized isolated rotors is lower for smaller-sized rotors when compared to coaxial rotorcraft in

Fig. 3. There is a difference of ~5.5k Watts for the required hover power between the coaxial rotorcraft and rotorcraft with 2 isolated rotors at a rotor size of 0.23 m diameter. Similar to the trends observed in the above-mentioned settings, the power required decreases exponentially and becomes approximately steady as the rotor diameter is increased. It is apparent that at the highest permitted rotor diameter of 4.5 m, the power is around ~2k Watts for all three configurations for hover, whereas, for the vertical climb, the conventional setting is more efficient as it requires noticeably lesser power than both coaxial and isolated settings.

6.5 Tandem Rotorcraft Analysis

Tandem rotorcraft can have numerous arrangements depending on the longitudinal positioning of the rotors on the top of the fuselage, thus, for the power consumption analysis three cases based on aeroshell structural extremities are analysed. Considering the fuselage length to be the size of the maximum aeroshell, i.e., 4.5 m, the two equal-sized rotors are equally placed at a displacement of 2.25 m, 1.125 m, and 0.75 m from the mid-point for Cases 1, 2 and 3, respectively, as depicted in Fig. 5. The rotors maximum diameter is 9 m in case 1, 4.5 m in case 2, and 3 m in case 3. Although in real design the clearance of rotor blades from the aeroshell inner walls and rotor hubs is mandatory, however, for this theoretical analysis such clearances are ignored. In all cases, when the diameter (D) of the rotor is equal to and less than half of the maximum diameter (D max), the overlapping of rotors disappears and therefore rotors theoretically act as isolated rotors. When the rotors become isolated in behavior, the rotorcraft theoretically becomes a multicopter design instead of a tandem rotor. Case 1 requires somewhat of an articulated rotor hub system with a folding mechanism to fit in the aeroshell for storage, Case 2 would require similar folding mechanics and an articulated rotor hub system if the D is above 2.25 m, whereas Case 3 can have a rigid (no linkages) rotor hub system. Table 2 provides the summary of the defined parameters of all three study cases for tandem rotorcraft.
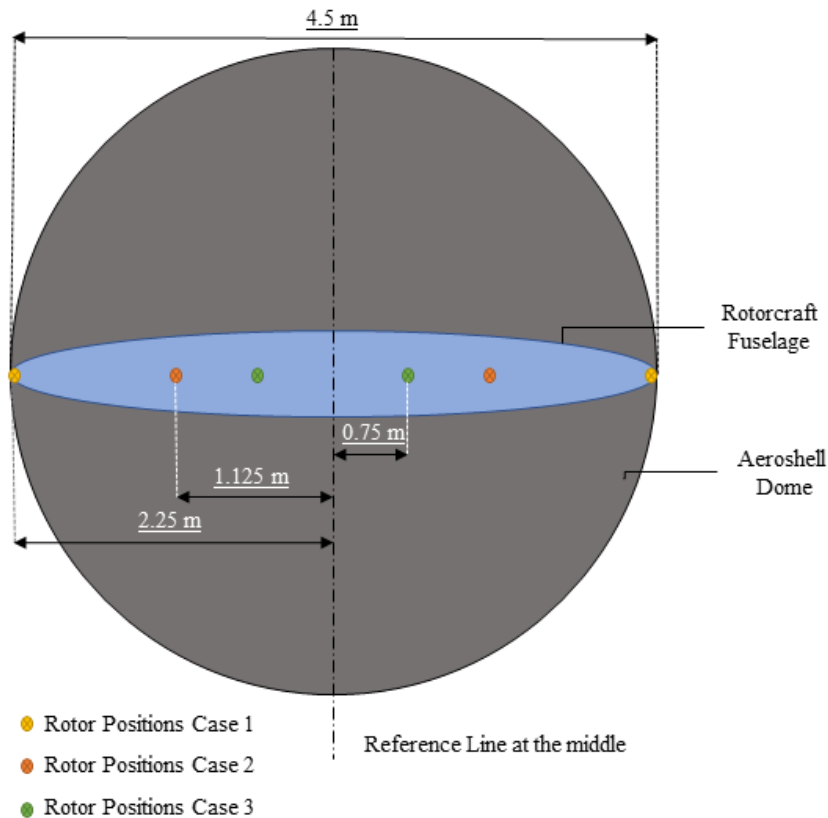

Fig. 5 Pictorial illustration of the rotor positioning of tandem rotorcraft cases 1, 2 and 3. (Not to scale)

Table 2   Summary of Tandem Rotorcraft Cases

Case No.	Rotor System Type	Folding Mechanism	Maximum Diameter	Rotor Position*	Isolated Rotor behaviour
1	Articulated	Yes	9 m	2.25 m	D ≤ 4.5 m
2	Articulated**	Yes**	4.5 m	1.125 m	D ≤ 2.25 m
3	Rigid	No	3 m	0.75 m	D ≤ 1.5 m

* Rotor hub position from the center of the fuselage

** When rotor D is > 2.25 m
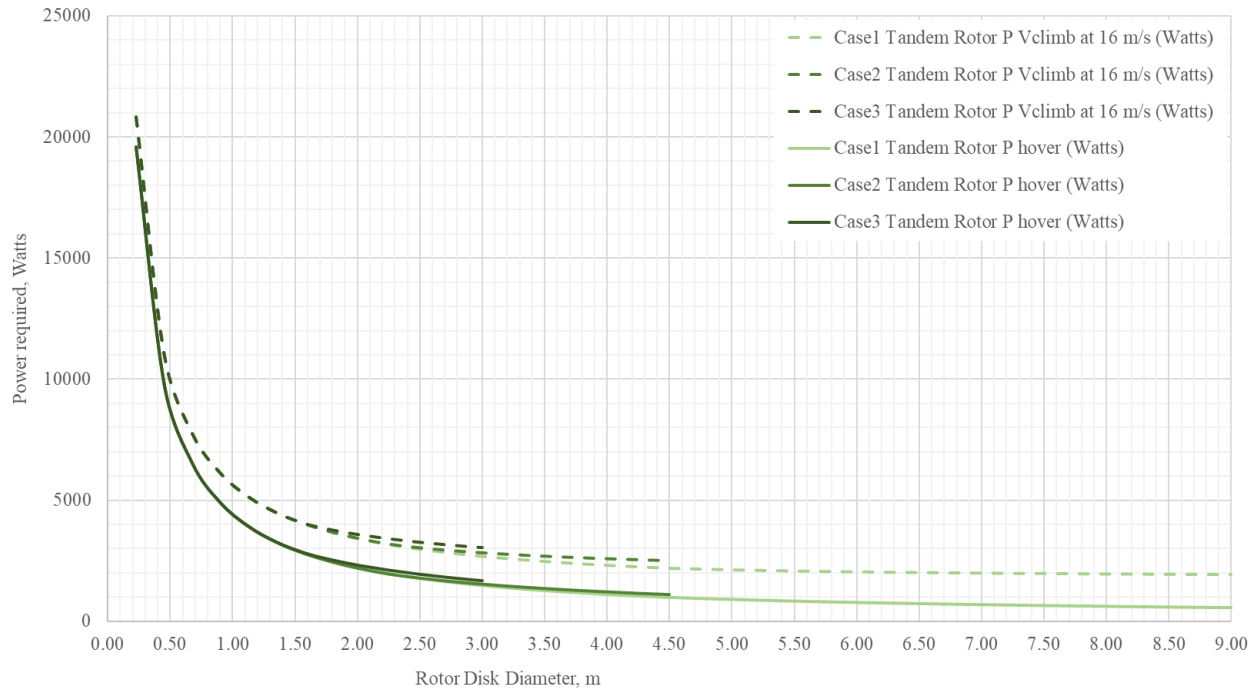
Fig. 6 20 kg Three Study Cases of Tandem Rotorcraft - Power Required Vs Rotor Disk Diameter (Area)

In Fig. 6 power required for all three study cases of tandem rotorcraft is plotted against the increasing rotor disk diameter. It can be observed that before any overlapping occurs between the rotors, the power required for the tandem rotorcraft system is the same as for isolated rotors. The overlapping interference factor (K_{ov}) is calculated using Eq. (3), for which the maximum K_{ov} is ~1.13 at 50% overlapping. The K_{ov} is 1 when there is no overlapping, however, this would need to be corrected as Eq. (3) would provide a range of values that are initially lower than 1 and then transition to above 1 as the rotor size decreases and the gap between the two rotors edges keeps diminishing. While the size of the rotor disk increases, the power required exponentially diminishes and the change becomes negligible as can be noticed in Case 1 for the rotor disk size values of 4.5 m to 9 m. However, when the tandem rotor power graph is compared to the coaxial rotor graph for smaller rotor sizes, the power consumption is considerably lower for the tandem rotorcraft.

6.6 Comparative Required Power Analysis of Different Rotor Configurations

Fig. 7 shows a comparison of power requirements for the hover and vertical climb of LS coaxial rotorcraft against the tandem rotorcraft Case 3. The K_{ov} of LS coaxial rotors is 1.3 whereas, for tandem rotor Case 3 with a maximum rotor diameter of 3 m (allowing maximum rotors overlapping of 50%), it is 1.13. The K_{ov} for Case 3 is reduced further when this overlapping is decreased for rotor disks of D<3 m. The difference of ~1000 Watts can be observed for hover power at 1.5 m D, where the tandem rotor has zero overlapping in this case. Thus, tandem rotor Case 3 can be considered a good configuration option as both hover and V_{climb} power efficiency are higher than the coaxial setting and is also mechanically

less complicated due to the rigid rotor hub system. For rotor disk sizes greater than 3 m, LS coaxial rotors can be considered but the penalty would be K_{ov} of 1.3, or the tandem rotor case 1 or 2 can be an option but the penalty would be an articulated hub system with a folding mechanism that adds complexity and weight to the overall system.

Fig. 8 and Fig. 9 show the graphical snapshot of hover power and V_{climb} power, respectively, against the rotor disk diameter of all the above-mentioned rotorcraft configurations. On the horizontal axis, the rotor disk diameter starts from 1 m for a zoomed-in observation in these graphs. The power required for 2 equal isolated rotors is stretched beyond 4.5 m rotor disk size only for analytic comparison with tandem rotor Case 1. Conventional helicopter requires the most power of all the configurations except in V_{climb} power, where it starts to consume less power than the other rotor configurations when the rotor size exceeds 2 m in diameter. One explanation of this fact is that a single helicopter rotor hub system contributes towards less forward/vertical flight profile drag, which makes it more efficient. However, larger rotor size also invites greater mechanical complexity, structural weight, and advancing blade tip shock waves.
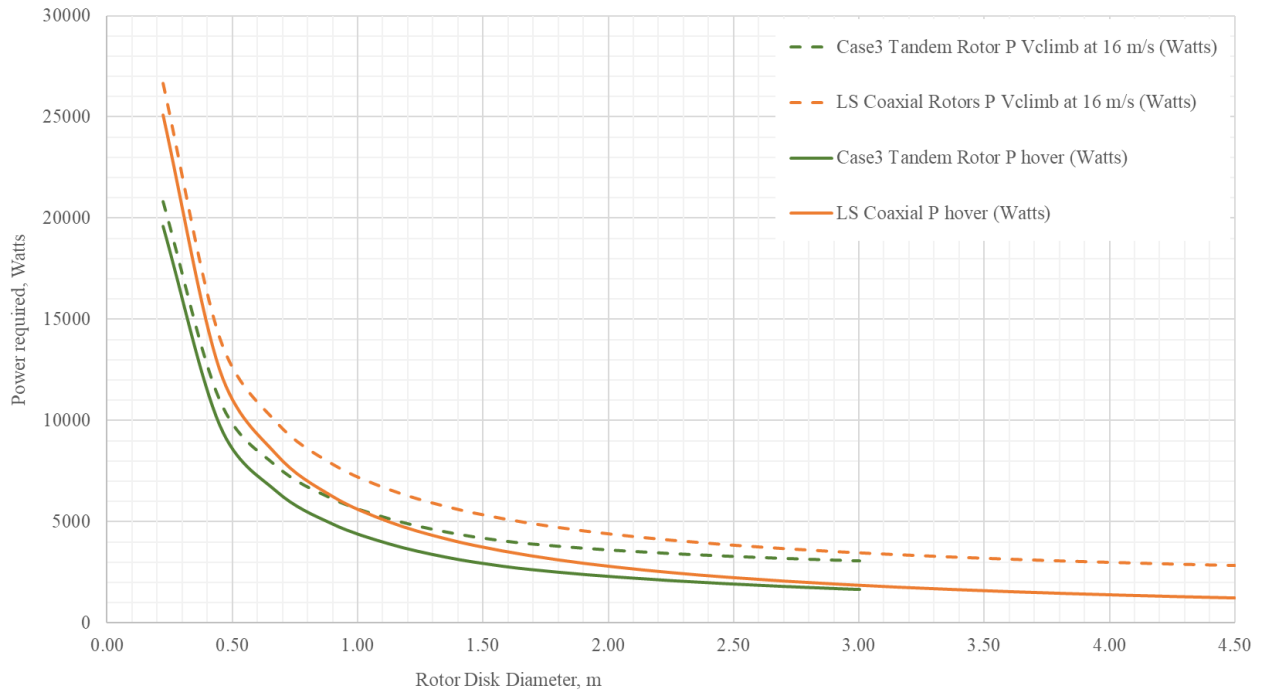

Fig. 7 20 kg Case 3 of Tandem Rotorcraft and LS Coaxial Rotorcraft - Power required Vs Rotor Disk Diameter (Area)
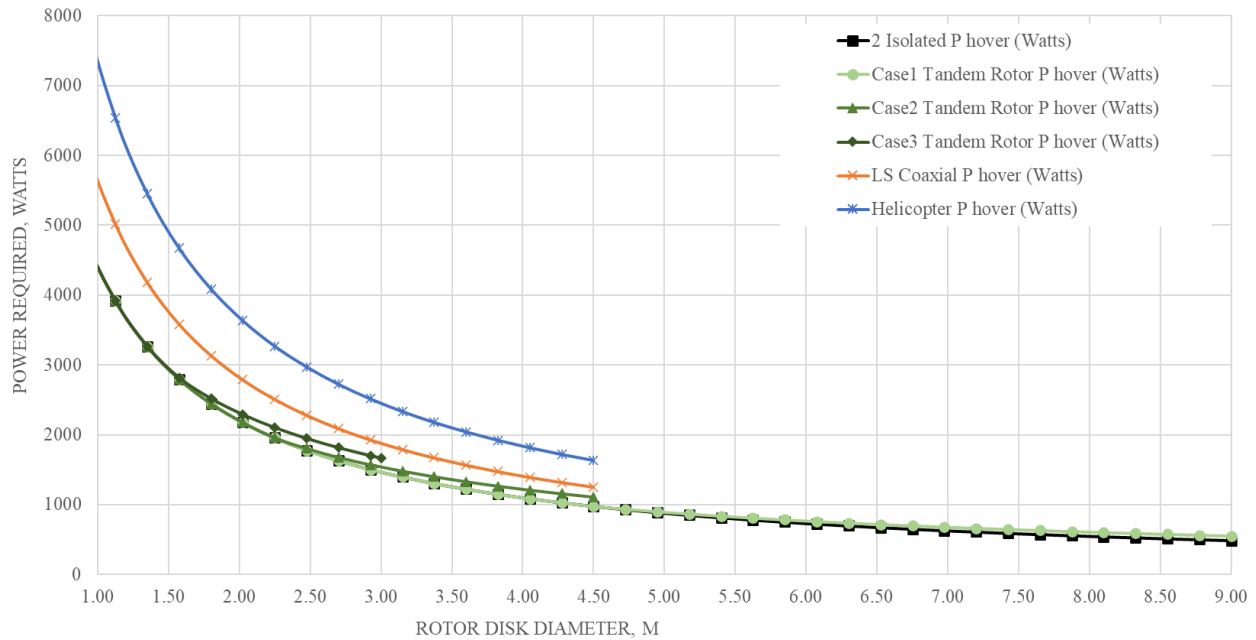
Fig. 8   Comparison between various 20 kg Rotorcraft configurations (Isolated, Tandem Cases, LS Coaxial, Helicopter) – Hover Power required Vs Rotor Disk Diameter (Area)
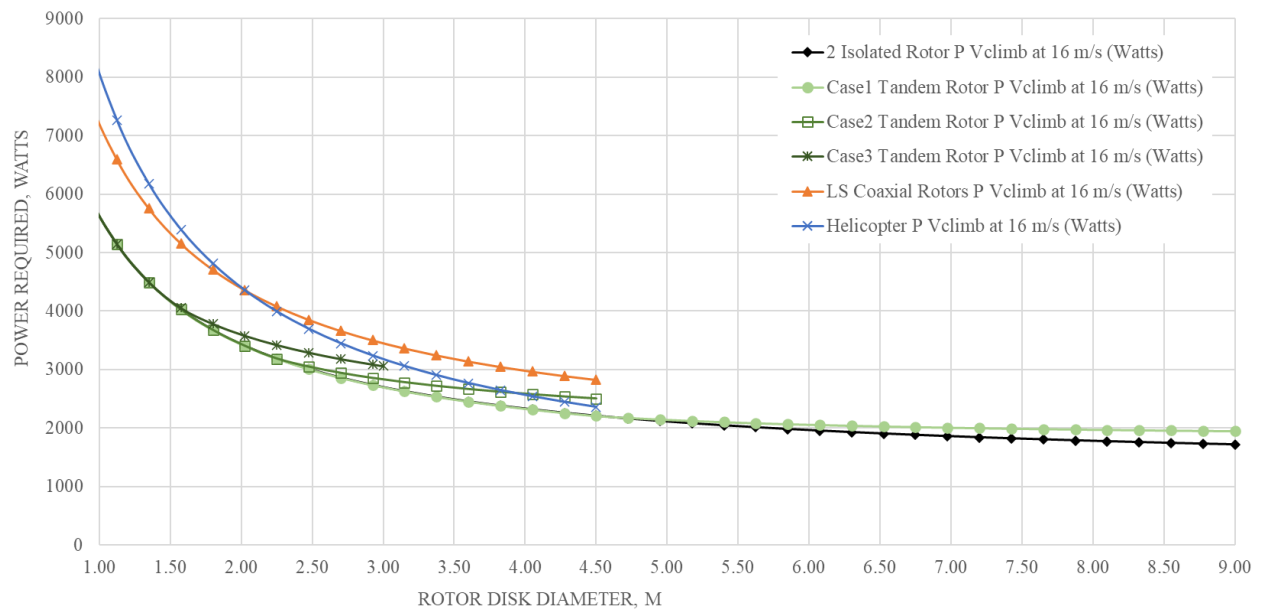
Fig. 9   Comparison between various 20 kg Rotorcraft configurations (Isolated, Tandem Cases, LS Coaxial, Helicopter) – Vertical climb Power required Vs Rotor Disk Diameter (Area)

6.7 Comparative V_{climb} BMF Analysis of Different Rotor Configurations

In Fig. 10 Battery Mass Fraction (BMF) of the calculated vertical climb required power for all the defined rotorcraft configurations is plotted against the increasing rotor disk diameter. The BMF is calculated for 1 min run time (E), a climb speed of 16 m/s and fixed total mass of 20 kg. The trend of V_{climb} BMF lines is similar to V_{climb} power dependency in Fig. 9.
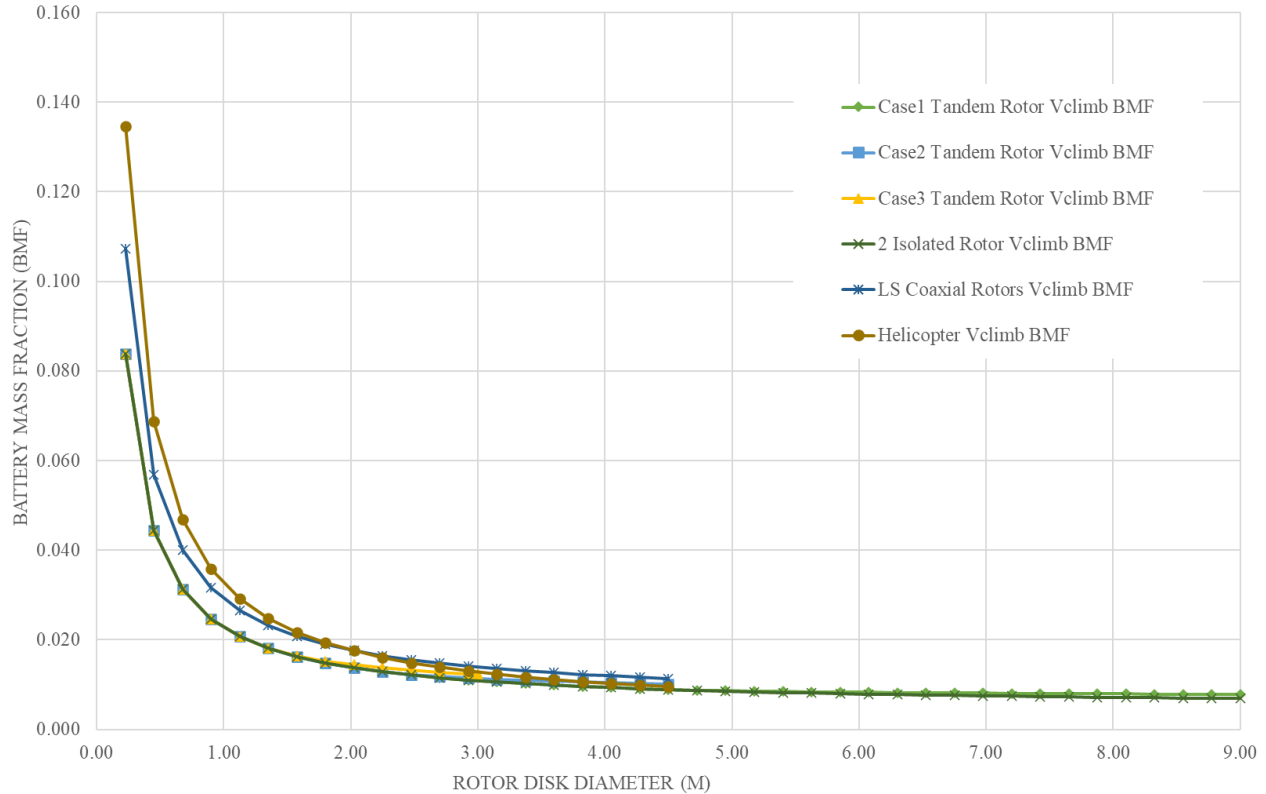

Fig. 10 20 kg Martian rotorcrafts – Vertical Climb BMF Vs Rotor Disk Diameter (Area)

The higher the required power the greater the BMF is, which reflects the required weight of the battery for this flight segment. The mass of the battery can simply be determined by multiplying the BMF with the total mass of the aircraft, e.g., for 0.02 BMF the mass of the battery equals 0.4 kg (i.e., 0.02 x 20 kg). BMF of each segment needs to be added up with the other flight segment, as explained in section 5, to calculate the total BMF and to find out the total battery mass needed for a particular flight regime. The BMF of forward flight or cruise is generally the highest of all segments because this would be the longest flight segment. Note that the BMF solved for the flight mission does not include the battery mass required for avionics or electronic payload instruments, as these would need to be calculated additionally unless these have separate dedicated batteries.

7. Conclusion

The first Mars Helicopter has proven that a rotorcraft can fly on Mars. Moving ahead from the gathered knowledge, future Mars rotorcrafts would require an upgraded solution. In this paper, we have specified the research gap and mission statement and defined basic parameters to proceed with the parametric study of various 20 kg rotorcraft configurations. The methodology is based on simplified helicopter momentum theory equations, which we have explained for each rotorcraft configuration and further derived with some estimates. Also, the methodology for the initial sizing of the battery-electric aircraft is introduced, which includes Battery Mass Fraction calculation for the flight segments to determine the required mass of the battery for flights. A graphical presentation of power required against increasing rotor disk diameter

is plotted for conventional helicopters, coaxial rotorcraft, tandem rotorcraft, and 2 isolated rotors rotorcraft. The conventional helicopter consumes higher hover power than all other configurations, whereas, for vertical climb power, the power required is higher for smaller rotors of size up to ~2 m, and above this size it considerably starts to decrease with increasing rotor size and becomes more efficient. Two isolated rotors are the ideal configuration as they do not have aerodynamic interference due to overlapping, and tandem rotors configuration achieves results closest to such settings. Tandem rotor Case 3 has proved to be an overall efficient configuration for a rotor disk size of up to 3 m when compared to the other configurations. The difference in power requirement between all configurations becomes negligible at a macro level for high rotor disk diameter (~4 m and above).

8. Future work

Based on the analysis and results, we have gathered estimates on the hover and vertical climb power consumptions of numerous Martian rotorcraft configurations. We are analyzing the power consumption of the forward flight of a rotorcraft with and without wings. In the follow-up work, we aim to extend this analytic research and provide a conclusive package with the pros and cons of various configurations based on their hover, vertical climb, and forward flight power consumption. We are optimistic that these analyses would help the Martian aerobot designer to select the most optimized configuration for a specific mission based on the theoretical estimates.

References

[1] Hassanalian, M., Rice, D., & Abdelkefi, A. Evolution of space drones for planetary exploration: A review. Progress in Aerospace Sciences, 97, 2018. 61–105. https://doi.org/10.1016/J.PAEROSCI.2018.01.003

[2] NASA. Overview | Mars – NASA Solar System Exploration. (2023) Retrieved May 25, 2023, from https://solarsystem.nasa.gov/planets/mars/overview/

[3] Radotich, M., Withrow-Maser, S., Gelhar, S., & Gallagher, H. (2021). A Study of Past, Present, and Future Mars Rotorcraft. 2021.

[4] Johnson, W., Withrow-Maser, S., Young, L., Malpica, C., Koning, W. J. F., Kuang, W., Fehler, M., Tuano, A., Chan, A., Datta, A., Chi, C., Lumba, R., Escobar, D., Balaram, J., Tzanetos, T., & Fjaer Grip, H. (2020). Mars Science Helicopter Conceptual Design. http://www.sti.nasa.gov

[5] NASA. (2023) Mars Helicopter - NASA Mars. Retrieved May 25, 2023, from https://mars.nasa.gov/technology/helicopter/#Flight-Log

[6] Young, L. A., Chen, R. T. N., Aiken, E. W., & Briggs, G. A. (2000). Design Opportunities and Challenges in the Development of Vertical Lift Planetary Aerial Vehicles.

[7] Aguirre, J., Casado, V., Chamie, N., & Zha, G. (2007). Mars Intelligent Reconnaissance Aerial and Ground Explorer (MIRAGE) AIAA 2007-244. https://doi.org/10.2514/6.2007-244

[8] Forshaw, J., & Lappas, V. (2012). Architecture and Systems Design of a Reusable Martian Twin Rotor Tailsitter. Acta Astronautica, 80(0), 166–180. https://doi.org/10.1016/J.ACTAASTRO.2012.05.008

[9] RM Zubrin. (2012). The mars gashopper - Concepts and Approaches for Mars 2012. https://ui.adsabs.harvard.edu/abs/2012LPICo1679.4069Z/abstract

[10] NASA. (2023) NASA TechPort - Project Data. Retrieved May 25, 2023, from https://techport.nasa.gov/view/93850

[11] Boelhouwer, R.N.J., Bunschoten, E.C., Debusscher, C.M.J., Frijters, W., van Goeverden, R.J., Legrand, E.B., Matton, J., Paliusis, K., and Verheyen, J.K.N. "Design Report, Martian Advanced Reconnaissance System." Delft University of Technology, June 2018.

[12] Underwood, C., & Collins, N. (2017). Design and Control of a Y-4 Tilt-Rotor VTOL Aerobot for Flight on Mars. Proceedings of the 68th International Astronautical Congress (IAC), 25–29. https://openresearch.surrey.ac.uk/esploro/outputs/conferencePresentation/Design-and-Control-of-a-Y-4-Tilt-Rotor-VTOL-Aerobot-for-Flight-on-Mars/99511131102346

[13] Denys, K. (2023) Ukrainian invention to feel the ground for Mars colonization (GRAPHICS) - Jun. 06, 2016 | KyivPost. Retrieved May 25, 2023, from https://www.kyivpost.com/article/content/ukraines-it-edge/ukrainian-invention-to-feel-the-ground-for-mars-colonization-graphics-415570.html

[14] Fathepure, M., Booker, A., Wang, N., Abouzahr, O., Tikalsky, D., Kheong Loh, W., & Jacob, J. D. (2021). Design and Construction of an Inflatable-Winged VTOL Mars Electric Flyer. https://doi.org/10.2514/6.2021-2578

[15] S. Withrow, W. Johnson, L. A. Young, H. Cummings, J. Balaram, and T. Tzanetos, "An Advanced Mars Helicopter Design," in ASCEND 2020, American Institute of Aeronautics and Astronautics.

[16] D. Raymer. Aircraft design: A conceptual approach, 6. Ed., AIAA education series, Reston, Va., 2018, Chaps. 20.11, 21.3.

[17] Leishman, J. Gordon. Principles of Helicopter Aerodynamics, 2. Ed., United Kingdom, Cambridge University Press, 2006. Chaps. 2.15, 5.5.11.

[18] Johnson, W. Rotorcraft Aeromechanics. Cambridge University Press. 2013. Chaps. 4.6, 5.3. https://doi.org/10.1017/CBO9781139235655

[19] NASA. (2023) Mars Fact Sheet. Retrieved May 03, 2023, from https://nssdc.gsfc.nasa.gov/planetary/factsheet/marsfact.html

[20] Climate Database (LMD/AOPP/IAA/ESA/CNES). http://www-mars.lmd.jussieu.fr/mars/mars.html Updated May 08, 2023. Accessed May 08, 2023.

[21] Balaram, J., Aung, M., Matthew, Golombek, P., Farley, K. A., Williford, K. H., Stack, K. M., Aung, M., & Golombek, M. P. The Ingenuity Helicopter on the Perseverance Rover. 2021. https://doi.org/10.1007/s11214-021-00815-w